ACS APPLIED ENERGY MATERIALS Letter
Cite This: ACS Appl. Energy Mater. XXXX, XXX, XXX−XXX
www.acsaem.org

Growth of AlGaAs, AlInP, and AlGaInP by Hydride Vapor Phase Epitaxy

Kevin L. Schulte,*[,†] Wondwosen Metaferia,[†] John Simon,[†] David Guiling,[†] Kevin Udwary,[‡] Gregg Dodson,[‡] Jacob H. Leach,[‡] and Aaron J. Ptak[†]

[†]National Renewable Energy Laboratory, Golden, Colorado 80401, United States
[‡]Kyma Technologies, Raleigh, North Carolina 27617, United States

ABSTRACT: We demonstrate hydride vapor phase epitaxy (HVPE) of $Al_xGa_{1-x}As$, $Al_xIn_{1-x}P$, and $Al_xGa_yIn_{1-x-y}P$ using an $AlCl_3$ precursor. We study the growth of the $Al_xGa_{1-x}As$ alloy system to elucidate the effects of deposition temperature, V/III ratio, and group V precursor species on Al solid incorporation via $AlCl_3$. Crucially, the presence of group V hydride at the growth front kinetically promotes the solid incorporation of Al. We use these insights to demonstrate controlled deposition of $Al_xGa_{1-x}As$, and for the first time by HVPE, $Al_xIn_{1-x}P$ and $Al_xGa_yIn_{1-x-y}P$. These results create exciting implications for HVPE-grown high-efficiency III−V solar cells and devices with reduced cost.

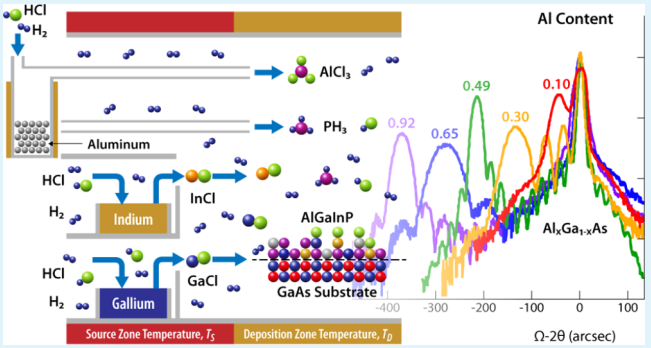

KEYWORDS: *solar energy, photovoltaics, III−V semiconductors, hydride vapor phase epitaxy, AlGaAs, AlInP, AlGaInP*

INTRODUCTION

Hydride vapor phase epitaxy (HVPE) is an epitaxial growth method with the potential to reduce deposition costs for III−V photovoltaics and other III−V optoelectronic devices.[1] Prior difficulties with the deposition of Al-containing III−V materials limited the ultimate performance of HVPE-grown devices, however.[2] Substitution of Al for Ga in GaAs and GaInP leads to a large increase in band gap but minimal change in lattice constant, providing a nearly independent knob to tune band gap while maintaining defect-free epitaxy. This property enables the formation of abrupt, high-quality heterobarriers that are vital to the performance of optoelectronic devices such as photovoltaics, transistors, and light emitting diodes. For example, $Al_{0.5}In_{0.5}P$ window layer passivation enables unmatched solar conversion efficiencies in high-efficiency III−V solar cells,[3] due to the material's large band gap that minimizes parasitic absorption in the front of the cell. Al-containing compounds can also serve as wide band gap active regions in multijunction solar cells,[4] with the Al solid fraction providing direct control over the device band gap. The ability to deposit Al-containing compounds by HVPE would have major implications on the outlook of this technology as a lower-cost replacement for incumbent metalorganic vapor phase epitaxy (MOVPE).

HVPE predates the development of MOVPE, the dominant III−V growth technique used in production today. From the 1970s to the 1980s, commercial production of light emitting diodes[5] and photodetectors and emitters for the telecommunications industry was achieved using HVPE.[6] HVPE was regarded as the best choice for creating materials with exceptional purity and electronic quality[7] but began to fall out of favor after the development of MOVPE in the 1980s for two main reasons. First, MOVPE enabled the formation of extremely abrupt heterointerfaces with ease, whereas HVPE historically struggled with heterointerfaces due to its high growth rates and the process inertia related to *in situ* generation of the group III precursors. This issue has largely been obviated in recent years with the advent of dynamic-HVPE,[1,8,9] a variant of the traditional HVPE growth technique. The second reason was HVPE's well-known difficulties with the deposition of Al-containing materials,[2] another growth aspect for which MOVPE was well-suited. Aluminum monochloride (AlCl), analogous to commonly utilized HVPE precursors GaCl and InCl, is highly unstable and etches quartz, requiring alumina or graphite reactor components.[10−14] Further complicating matters, attempts to grow Al-containing compounds from AlCl required growth temperatures of up to 1000 °C to suppress predeposition.[2] Large differences in the thermodynamics of the growth of GaAs and AlAs precluded the formation of $Al_xGa_{1-x}As$ alloys from GaCl and AlCl; rather, only binary phases could be formed.[11,15] Figure 1 plots the equilibrium constant, K_{eq}, for the growth of GaAs and AlAs from various group III precursors and As_4 or AsH_3 group V precursors, calculated from the thermochemical data in ref 16. These calculations neglect to include equilibrium between other gas phase precursors, but the trends are still instructive. The large K_{eq} for the growth of AlAs from AlCl implies a large driving force for the deposition of

Received: October 21, 2019
Accepted: December 5, 2019

DOI: 10.1021/acsaem.9b02080
ACS Appl. Energy Mater. XXXX, XXX, XXX−XXX

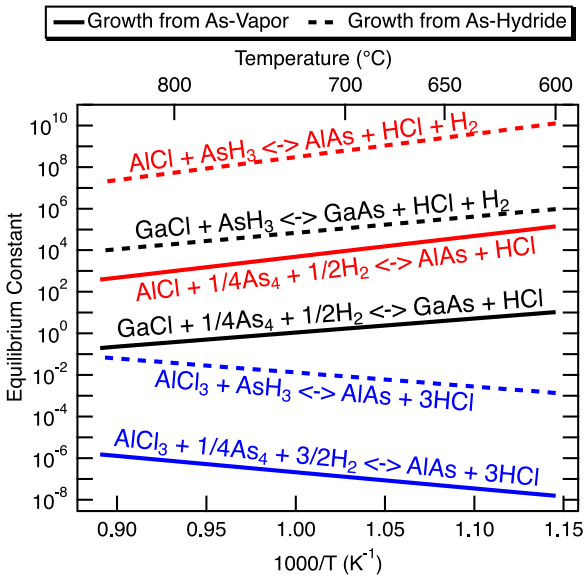

Figure 1. Plot of the equilibrium constant for deposition of solid AlAs and GaAs using various group III precursors and As vapor (As_4) or As hydride (AsH_3).

this material, hence the difficulty controlling its growth at temperatures below 1000 °C. These temperatures are also not conducive to the incorporation of relatively volatile In into Al-containing alloys, which precludes the possibility of growing Al(Ga)InP. Eventually, researchers did demonstrate $Al_xGa_{1-x}As$ growth by HVPE, but only by using a mixed Ga/Al source.[13,14,17] Differences in Al and Ga depletion rates in the melt lead to a drifting solid composition, however, making commercial production challenging with this method. In large part due to these difficulties, MOVPE became the dominant technique for III−V optoelectronic device production.

Aluminum monochloride is not the only possible Al-containing HVPE precursor, however. Aluminum trichloride, $AlCl_3$, is significantly more stable than AlCl and does not readily react to form AlAs, as demonstrated by the miniscule equilibrium constant for deposition of AlAs from $AlCl_3$ shown in Figure 1. This stability similarly limits reaction of $AlCl_3$ with heated quartz reactor components.[18] Despite the low driving force for solid deposition directly from $AlCl_3$ indicated in Figure 1, various reports throughout the late 1980s and early 1990s demonstrated that the growth of AlAs and $Al_xGa_{1-x}As$ by HVPE was possible at temperatures as low as 500 °C using $AlCl_3$.[19−22] Growth of an Al-containing compound at those temperatures is highly promising for the deposition of Al(Ga)InP. To date, we are aware of no reports of growth of Al phosphide materials by HVPE.

$AlCl_3$ is a solid below ∼195 °C and has a low vapor pressure at room temperature. Thus, a heated $AlCl_3$ source and process lines are required to transport this precursor with an inert carrier, an embodiment used by some groups.[21,22] However, this method is limited in the molar flow rate that it can deliver at standard line temperatures and bubbler flows. An alternative method is to generate $AlCl_3$ from solid Al and HCl, a method commonly used to facilitate HVPE of III−N materials.[18,23−25] Thermodynamic calculations indicate that formation of $AlCl_3$ from HCl and solid Al is favored over AlCl at temperatures below ∼700 °C, with $AlCl_3$ selectivity increasing as the Al source temperature is reduced.[18] These same predictions suggest that the problematic AlCl could form as a byproduct of $AlCl_3$ decomposition in hotter sections of the reactor downstream if decomposition kinetics are fast enough. However, there is evidence from high-temperature (≥1000 °C) Al nitride growth that, once generated in a lower-temperature source region, the $AlCl_3$ molecule can pass through hotter regions of the reactor with limited decomposition.[24] $AlCl_3$ generation can be accomplished *in situ*[18,20] or *ex situ*, with the latter providing increased flexibility in the design of the quartz reaction vessel.

In this work, we demonstrate the deposition of multiple types of Al-containing III−V materials by HVPE using an $AlCl_x$ generator. We select for $AlCl_3$ through use of a 400 °C source temperature, enabling controlled incorporation of Al in the solid phase. We verify that the $AlCl_3$ molecule is resistant to decomposition in a typical range of temperatures employed in our reactor. We study the growth of the $Al_xGa_{1-x}As$ alloy system to understand the effects of growth conditions such as growth temperature, V/III ratio, and group V species on Al

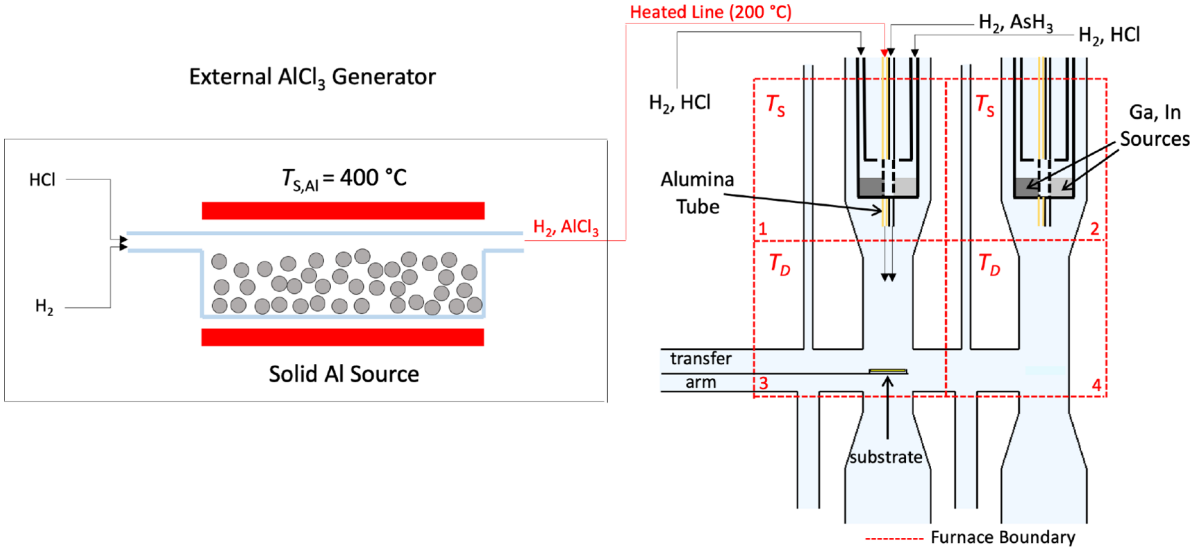

Figure 2. Diagram of the dynamic HVPE reactor used in this study, including the external $AlCl_3$ generator (not to scale).

DOI: 10.1021/acsaem.9b02080
ACS Appl. Energy Mater. XXXX, XXX, XXX−XXX

incorporation from the $AlCl_3$ precursor. Our results show that use of group V hydride, such as AsH_3, instead of group V vapor, such as As_2/As_4, promotes stronger Al incorporation. We extend this understanding gleaned from $Al_xGa_{1-x}As$ growth to demonstrate the growth of $Al_xIn_{1-x}P$ and $Al_xGa_yIn_{1-x-y}P$ for the first time by HVPE, an undertaking once thought to be infeasible.[26,27] These results enable the deposition of high-efficiency solar cell designs previously unattainable by HVPE.

EXPERIMENTAL SECTION

Materials were grown in our atmospheric pressure, dual-chamber HVPE reactor[9] shown schematically in Figure 2. GaCl and InCl were generated *in situ* from HCl and elemental Ga and In in the upper half of each reactor chamber. The Ga and In source temperatures in zones 1 and 2, denoted T_S, were 800 °C, except where otherwise stated in this paper. Substrates were (100)-oriented GaAs with an offcut of 6° toward the (111)A plane. $AlCl_3$ was generated *ex situ* in a separate quartz boat enclosed in a clamshell furnace. The Al furnace temperature, $T_{S,Al}$, was 400 °C in order to promote generation of $AlCl_3$ instead of AlCl.[18] Al precursor generation was controlled by the flow rates of HCl and H_2 carrier to the boat as indicated in Figure 2. The process lines that deliver the Al precursor to the reactor were heated to 200 °C using insulated heat tapes to prevent solidification of the $AlCl_3$ and subsequent clogging of the lines. The Al line is plumbed into the reactor through an alumina tube that extends through the majority of the 800 °C upper source zones. The alumina tube is inert to reaction with $AlCl_3$ or decomposition byproducts and has an inner diameter of 4 mm to promote a high precursor velocity through the higher-temperature source zone.

GaAs/$Al_xGa_{1-x}As$/GaAs structures were grown and analyzed for Al solid content (x_{Al}) and $Al_xGa_{1-x}As$ growth rate (R_G). The deposition temperature (T_D) in zones 3 and 4 was 650 °C except where otherwise noted. The total H_2 flow rate was ~8500 sccm, with the flow rates of the other precursors noted later in the figures. AsH_3 was the group V precursor input to the reactor, with the extent of decomposition of this precursor into As_x species controlled by its H_2 carrier flow rate. The $Al_xGa_{1-x}As$ lattice constant was measured using high-resolution X-ray diffraction and used to compute x_{Al} following ref 28. Epilayer thickness and growth rate were determined by fitting the sample reflectance using a transfer matrix method[29] incorporating refractive index and absorption coefficient data calculated from ref 30. $Al_xIn_{1-x}P$ and $Al_xGa_yIn_{1-x-y}P$ epilayers were grown at a temperature of 650 °C from $AlCl_3$, InCl, GaCl, and PH_3. The composition of the quaternary alloy was determined through measurement of the lattice constant by X-ray diffraction and band gap determination from spectroscopic transmission measurements. Transmission samples were fabricated by bonding the epilayer side to a glass handle with transparent epoxy and selectively etching away the absorbing substrate using an ammonium hydroxide/hydrogen peroxide based etchant.

RESULTS AND DISCUSSION

We performed two experiments to verify that the precursor generated in the Al source, and the one that eventually reaches the growth front, is $AlCl_3$. First, we varied the deposition temperature, T_D, under constant reactor flows and constant upper zone 1 and 2 temperatures (T_S). Figure 3 shows x_{Al} and the growth rate for this series of samples. x_{Al} increases strongly with T_D, and the growth rate varies weakly, passing through a maximum near 650 °C. The trend of increasing x_{Al} with T_D agrees with the equilibrium curves in Figure 1, which predict that the driving force for AlAs growth from $AlCl_3$ increases with T_D while the driving force for GaAs growth from GaCl simultaneously decreases. The growth rate is relatively insensitive in this temperature range because of these opposite trends in K_{eq} for each binary. This result suggests that $AlCl_3$ is the dominant Al precursor in the reactor, because growth from

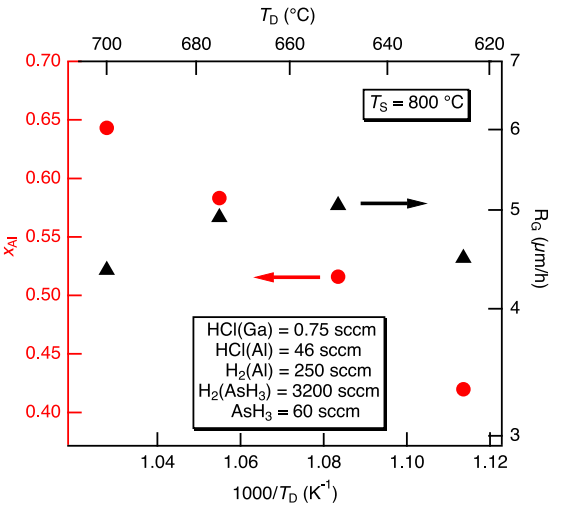

Figure 3. x_{Al} (left axis) and growth rate (right axis) of $Al_xGa_{1-x}As$ epilayers grown with varying deposition temperature (T_D) at constant source temperature (T_S).

AlCl and GaCl is expected to exhibit a monotonic growth rate decrease based on Figure 1. We also note that the large HCl(Al)/HCl(Ga) ratio of 61 needed to achieve x_{Al} = 0.4−0.6 suggests that the species reaching the substrate surface is $AlCl_3$. The more reactive AlCl would be expected to completely overwhelm Ga incorporation in the film at that ratio, as indicated in Figure 1.

Next, we varied T_S using constant reactant flows with constant T_D to determine whether this would alter the distribution of $AlCl_x$ species in the reactor. Changing T_S is a useful method to alter the chemistry within the reactor independent of T_D or reactant flows. In previous work, we used this method to affect the decomposition of AsH_3 in the reactor.[31] Figure 4 displays the results of a similar experiment studying the effect of T_S on $Al_xGa_{1-x}As$ growth. x_{Al} is relatively constant as T_S varies between 650 and 800 °C. The growth rate is also relatively constant until it shows a decrease at T_S = 800 °C. It is possible that AsH_3 decomposition increased at the

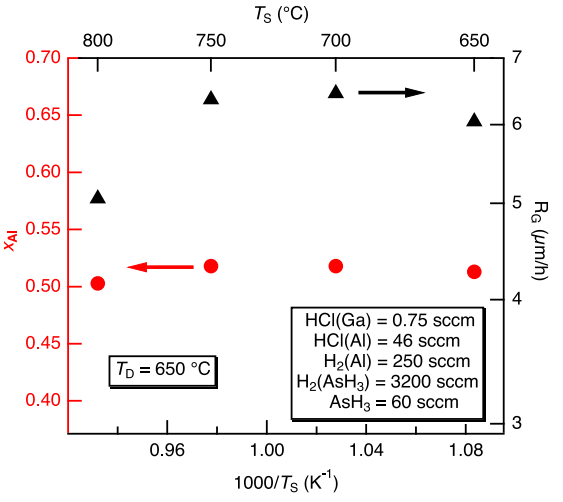

Figure 4. x_{Al} (left axis) and growth rate (right axis) of $Al_xGa_{1-x}As$ epilayers grown with varying source temperature (T_S) at constant deposition temperature (T_D). All other growth parameters were held constant.

DOI: 10.1021/acsaem.9b02080
ACS Appl. Energy Mater. XXXX, XXX, XXX−XXX

highest temperature and led to decreased growth rate as suggested by the results in ref 31. The insensitivity of x_{Al} and the growth rate to T_S imply that the Al precursor distribution is not affected in this temperature range, at least in conjunction with the injection scheme used here. This result, combined with the result of the first experiment, strongly suggests that the predominant Al growth species in the reactor is $AlCl_3$ and that it is not substantially decomposing to AlCl at typical reactor temperatures.

We then investigated the effects of the both the flow rate and the nature of the group V precursor on $Al_xGa_{1-x}As$ growth. Figure 5 shows the effect of AsH_3 flow rate on x_{Al} and the

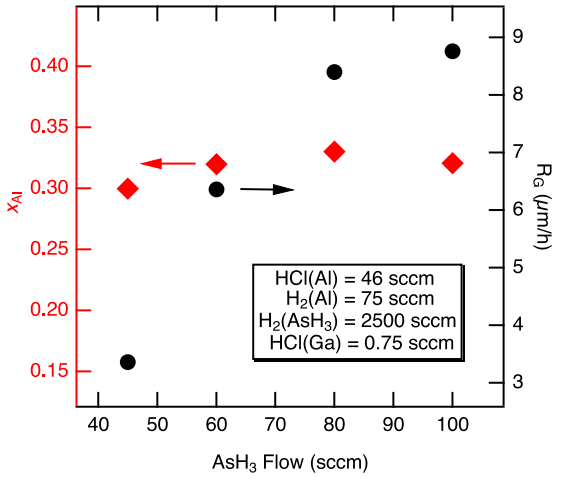

Figure 5. x_{Al} (left axis) and $Al_xGa_{1-x}As$ growth rate (right axis) as a function of AsH_3 flow rate in epilayers grown with T_D = 650 °C and all other parameters constant.

growth rate. We see that x_{Al} is roughly constant as the AsH_3 flow rate is increased from 45 to 100 sccm. However, the growth rate more than doubles within this range, implying that the increased AsH_3 flow rate is increasing both Ga and Al incorporation in the solid because of the relative insensitivity of x_{Al} to this parameter. The identity of the group V species has a much stronger effect on $Al_xGa_{1-x}As$ growth. In a previous study, we showed that the GaAs growth rate could be enhanced by limiting decomposition of the AsH_3 precursor into As_2/As_4.[31] In that work, we limited AsH_3 decomposition by increasing the flow rate of H_2 carrier input with the AsH_3, which increases the velocity of the AsH_3 through the reactor and decreases the amount of time it spends in the higher-temperature 800 °C source zone where it would quickly decompose. Figure 6 shows x_{Al} and growth rate for a series of $Al_xGa_{1-x}As$ samples grown with varying AsH_3 carrier flow rate. Note that the carrier flow rate was compensated in another reactor port so that the total H_2 flow rate and reactant dilution level were constant. x_{Al} increases strongly with the AsH_3 carrier flow rate, and the growth rate increases as well. These results imply that the presence of uncracked AsH_3 is key to the incorporation of Al in the solid, as similarly found for AlAs growth.[22] This can be understood by considering that K_{eq} for growth of AlAs from $AlCl_3$ and As_4 is extremely low, as seen in Figure 1, while K_{eq} for AlAs growth from $AlCl_3$ and AsH_3 is nearly 5 orders of magnitude larger.[16] We further note that K_{eq} for AlAs growth from $AlCl_3$ and AsH_3 is still well below unity at 650 °C, however, indicating that the equilibrium calculations do not tell the entire story. It is likely that the presence of

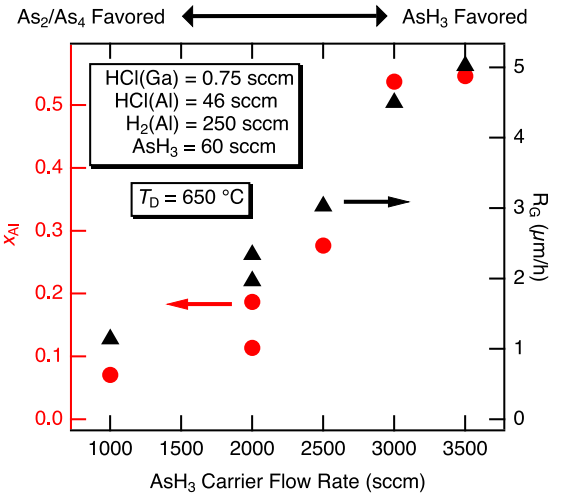

Figure 6. x_{Al} (left axis) and $Al_xGa_{1-x}As$ growth rate (right axis) as a function of AsH_3 carrier flow rate in epilayers grown with T_D = 650 °C and all other parameters constant.

unreacted AsH_3 modifies the kinetics at the substrate surface, enhancing Al incorporation from the $AlCl_3$. AsH_3 that decomposes on the substrate surface may provide reactive H radicals that help drive the kinetic reduction of the otherwise highly stable $AlCl_3$ molecule, explaining the trends observed in Figure 6.

Thus, the use of $AlCl_3$ allows for the controlled deposition of Al containing compounds by HVPE, enabling new applications for the technique. Using the understanding developed in the $Al_xGa_{1-x}As$ growth studies, we can achieve $Al_xGa_{1-x}As$ with x_{Al} tunable between 0 and 1. Figure 7 shows (004) X-ray

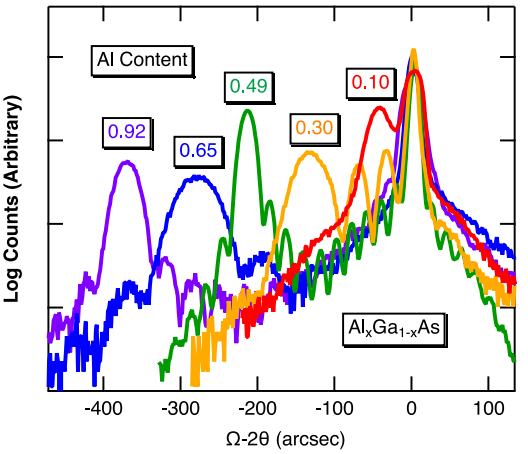

Figure 7. (004) Ω−2Θ high resolution X-ray diffraction scans of $Al_xGa_{1-x}As$ epilayers nearly spanning the entire compositional space.

diffraction curves for samples with Al content varying from 0.10 to 0.92. Use of the $AlCl_3$ precursor is extendable to deposition of Al phosphide compounds by HVPE, for which we are aware of no prior reports of growth by this technique. Figure 8 shows optical transmission measurements of (a) $Al_xIn_{1-x}P$ and (b) $Al_xGa_yIn_{1-x-y}P$ epilayers with compositions closely lattice-matched to GaAs. The direct band gaps were obtained by fitting the linear region of the absorption edge. These wide band gap epilayers are extremely useful in many III−V devices. For example, they can be readily integrated into solar cells[3] to provide transparent passivation for front and rear

DOI: 10.1021/acsaem.9b02080
ACS Appl. Energy Mater. XXXX, XXX, XXX−XXX

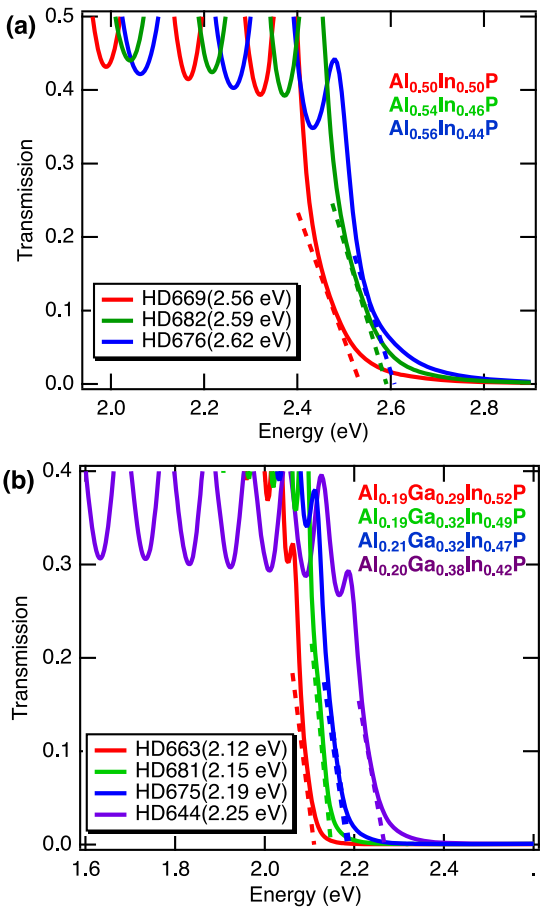

Figure 8. Transmission spectra of (a) $Al_xIn_{1-x}P$ and (b) Al_xGa_y-$In_{1-x-y}P$ epilayers bonded to glass.

surfaces, or as the active layers in LED devices that emit at green wavelengths.[32] Figure 9 shows x_{Al} for $Al_xIn_{1-x}P$ epilayers grown near the lattice-matched composition as a function of $AlCl_3$/InCl ratio. Near unity $AlCl_3$/InCl ratios are necessary to achieve a 50/50 solid composition, making the growth of $Al_xIn_{1-x}P$ not only possible but readily controllable, in stark contrast to growth via AlCl. The inset of Figure 9 shows an (004) X-ray diffraction curve of a 20 nm thick lattice-matched $Al_{0.53}In_{0.47}P$ layer. The appearance of Pendellosung fringes indicates that the growth is epitaxial and highly planar. The growth of phosphide materials by HVPE opens up exciting possibilities for the deposition of high-efficiency III−V photovoltaics with reduced cost.

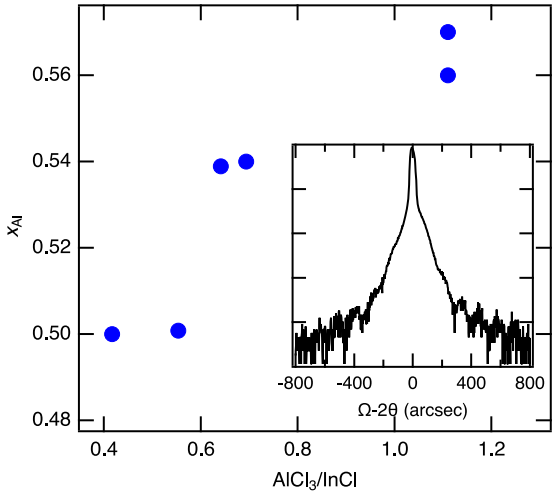

Figure 9. x_{Al} in $Al_xIn_{1-x}P$ for epilayers grown nearly lattice-matched to GaAs as a function of $AlCl_3$/InCl ratio, assuming complete conversion of HCl to MCl_x. Inset: (004) X-ray diffraction curve of a 20 nm thick $Al_{0.53}In_{0.47}P$ layer grown on a GaAs substrate.

CONCLUSION

We demonstrated a method for the controlled deposition of Al-containing III−V materials by HVPE through *ex situ* generation of $AlCl_3$. We selected for $AlCl_3$ instead of AlCl in the $AlCl_x$ generation reaction through use of a 400 °C source temperature. We showed that the $AlCl_3$ molecule was resistant to decomposition at typical source and deposition temperatures in our reactor. We studied growth of the $Al_xGa_{1-x}As$ alloy system to elucidate the effects of growth conditions such as deposition temperature, V/III ratio, and group V species on Al incorporation from $AlCl_3$. We found that conditions that select for the group V hydride over the group V vapor strongly promoted incorporation of Al in the film. Using these insights, we demonstrated control over $Al_xGa_{1-x}As$ composition in the entire range x_{Al} = 0−1, as well as the growth of $Al_xIn_{1-x}P$ and $Al_xGa_yIn_{1-x-y}P$ for the first time by HVPE. These results have exciting implications for the growth of new high-performance photovoltaics and other optoelectronic devices by HVPE with reduced cost.

AUTHOR INFORMATION

Corresponding Author

*E-mail: kevin.schulte@nrel.gov.

ORCID

Kevin L. Schulte: 0000-0003-4273-6254

Author Contributions

The manuscript was written through contributions of all authors. All authors have given approval to the final version of the manuscript.

Notes

The authors declare no competing financial interest.

ACKNOWLEDGMENTS

The authors wish to thank Evan Wong for assistance processing the transmittance samples and Al Hicks for assistance with the table of contents graphic. This work was authored by Alliance for Sustainable Energy, LLC, the manager and operator of the National Renewable Energy Laboratory for the U.S. Department of Energy (DOE) under Contract DE-AC36-08GO28308. This material is based upon work supported by the U.S. Department of Energy's Office of Energy Efficiency and Renewable Energy (EERE) under Solar Energy Technologies Office (SETO) Agreement Numbers 30290 and 34358. The views expressed in the article do not necessarily represent the views of the DOE or the U.S. Government. The U.S. Government retains and the publisher, by accepting the article for publication, acknowledges that the U.S. Government retains a nonexclusive, paid-up, irrevocable, worldwide license to publish or reproduce the published form of this work, or allow others to do so, for U.S. Government purposes.

DOI: 10.1021/acsaem.9b02080
ACS Appl. Energy Mater. XXXX, XXX, XXX−XXX

REFERENCES

(1) Simon, J.; Schulte, K.; Horowitz, K.; Remo, T.; Young, D.; Ptak, A. III-V-Based Optoelectronics with Low-Cost Dynamic Hydride Vapor Phase Epitaxy. *Crystals* **2019**, *9* (1), 3.

(2) Stringfellow, G. VPE growth of III/V semiconductors. *Annu. Rev. Mater. Sci.* **1978**, *8* (1), 73−98.

(3) Olson, J.; Kurtz, S.; Kibbler, A.; Faine, P. A 27.3% efficient Ga0. 5In0. 5P/GaAs tandem solar cell. *Appl. Phys. Lett.* **1990**, *56* (7), 623−625.

(4) Geisz, J. F.; Steiner, M. A.; Jain, N.; Schulte, K. L.; France, R. M.; McMahon, W. E.; Perl, E. E.; Friedman, D. J. Building a six-junction inverted metamorphic concentrator solar cell. *IEEE J. Photovoltaics* **2018**, *8* (2), 626−632.

(5) Bhargava, R. Recent advances in visible LED's. *IEEE Trans. Electron Devices* **1975**, *22* (9), 691−701.

(6) Ban, V.; Popov, M.; Erickson, G.; Speer, F.; Gay, D.; Olsen, G. In *VPE Growth Of InGaAs For Large Area And Extended Spectral Range Photodetectors*; Components for Fiber Optic Applications; International Society for Optics and Photonics, 1987; pp 192−199.

(7) Abrokwah, J.; Peck, T.; Walterson, R.; Stillman, G.; Low, T.; Skromme, B. High purity GaAs grown by the hydride vpe process. *J. Electron. Mater.* **1983**, *12* (4), 681−699.

(8) Schulte, K. L.; Simon, J.; Ptak, A. J. Multijunction $Ga_{0.5}In_{0.5}P$/GaAs solar cells grown by dynamic hydride vapor phase epitaxy. *Prog. Photovoltaics* **2018**, *26* (11), 887−893.

(9) Metaferia, W.; Schulte, K. L.; Simon, J.; Johnston, S.; Ptak, A. J. Gallium arsenide solar cells grown at rates exceeding 300 μm h− 1 by hydride vapor phase epitaxy. *Nat. Commun.* **2019**, *10* (1), 3361.

(10) Johnston, W. D. Vapor-phase-epitaxial growth of n-AlAs/p-GaAs solar cells. *J. Cryst. Growth* **1977**, *39* (1), 117−127.

(11) Ettenberg, M.; Sigai, A.; Dreeben, A.; Gilbert, S. Vapor Growth and Properties of AlAs. *J. Electrochem. Soc.* **1971**, *118* (8), 1355−1358.

(12) Sigai, A.; Abrahams, M.; Blanc, J. Properties of Vapor-Deposited Aluminum Arsenide. *J. Electrochem. Soc.* **1972**, *119* (7), 952−956.

(13) Bachem, K.-H.; Heyen, M. Conditions for VPE growth of AlxGa1− xAs alloys in inorganic transport systems. *J. Cryst. Growth* **1981**, *55* (2), 330−338.

(14) Deschler, M.; Cuppers, M.; Brauers, A.; Heyen, M.; Balk, P. Halogen VPE of AlGaAs for optoelectronic device applications. *J. Cryst. Growth* **1987**, *82* (4), 628−638.

(15) Johnston, W.; Callahan, W. VPE Growth of n-AlAs on GaAs for Heterojunction Devices. *J. Electrochem. Soc.* **1976**, *123* (10), 1524−1531.

(16) Barin, I. *Thermochemical Data of Pure Substances*, 3rd ed.; VCH, 1995.

(17) Bachem, K.; Heyen, M. In *Epitaxial Growth of AlxGa1-xAs in a Chloride Transport System*; Institute of Physics Conference Series No. 56; Institute of Physics, 1980; Chapter 1.

(18) Kumagai, Y.; Yamane, T.; Miyaji, T.; Murakami, H.; Kangawa, Y.; Koukitu, A. Hydride vapor phase epitaxy of AlN: thermodynamic analysis of aluminum source and its application to growth. *Phys. Status Solidi C* **2003**, *0* (7), 2498−2501.

(19) Hasegawa, F.; Yamamoto, T.; Katayama, K.; Nannichi, Y. Vapor phase epitaxial growth of AlAs by chloride transport method. *J. Electrochem. Soc.* **1987**, *134* (6), 1548−1553.

(20) Hasegawa, F.; Katayama, K.; Kobayashi, R.; Yamaguchi, H.; Nannichi, Y. Chloride VPE of AlxGa1-xAs by the Hydrogen Reduction Method Using a Metal Al Source. *Japanese journal of applied physics* **1988**, *27* (2A), L254.

(21) Yamaguchi, H.; Kobayashi, R.; Jin, Y.; Hasegawa, F. Vapor Phase Epitaxy of AlGaAs by Direct Reaction between AlCl3, GaCl3 and AsH3/H2. *Jpn. J. Appl. Phys.* **1989**, *28* (1A), L4.

(22) Kobayashi, R.; Jin, Y.; Hasegawa, F.; Koukitu, A.; Seki, H. Low temperature growth of GaAs and AlAs by direct reaction between GaCl3, AlCl3 and AsH3. *J. Cryst. Growth* **1991**, *113* (3−4), 491−498.

(23) Baker, T.; Mayo, A.; Veisi, Z.; Lu, P.; Schmitt, J. Hydride vapor phase epitaxy of AlN using a high temperature hot-wall reactor. *J. Cryst. Growth* **2014**, *403*, 29−31.

(24) Koukitu, A.; Kumagai, Y.; Marui, T. Vapor phase growth method for Al-containing III-V group compound semiconductor, and method and device for producing Al-containing III-V group compound semiconductor. US 7,645,340 B2, January 12, 2010, 2010.

(25) Hagedorn, S.; Richter, E.; Zeimer, U.; Prasai, D.; John, W.; Weyers, M. HVPE of AlxGa1− xN layers on planar and trench patterned sapphire. *J. Cryst. Growth* **2012**, *353* (1), 129−133.

(26) Yuan, J.; Hsu, C.; Cohen, R.; Stringfellow, G. Organometallic vapor phase epitaxial growth of AlGaInP. *J. Appl. Phys.* **1985**, *57* (4), 1380−1383.

(27) Stringfellow, G. OMVPE growth of AlxGa1− xAs. *J. Cryst. Growth* **1981**, *55* (1), 42−52.

(28) Zhou, D.; Usher, B. F. Deviation of the AlGaAs lattice constant from Vegard's law. *J. Phys. D: Appl. Phys.* **2001**, *34* (10), 1461.

(29) Katsidis, C. C.; Siapkas, D. I. General transfer-matrix method for optical multilayer systems with coherent, partially coherent, and incoherent interference. *Appl. Opt.* **2002**, *41* (19), 3978−3987.

(30) Adachi, S. Optical properties of Al x Ga 1− x As alloys. *Phys. Rev. B: Condens. Matter Mater. Phys.* **1988**, *38* (17), 12345.

(31) Schulte, K. L.; Braun, A.; Simon, J.; Ptak, A. J. High growth rate hydride vapor phase epitaxy at low temperature through use of uncracked hydrides. *Appl. Phys. Lett.* **2018**, *112* (4), 042101.

(32) Streubel, K.; Linder, N.; Wirth, R.; Jaeger, A. High brightness AlGaInP light-emitting diodes. *IEEE J. Sel. Top. Quantum Electron.* **2002**, *8* (2), 321−332.

DOI: 10.1021/acsaem.9b02080
ACS Appl. Energy Mater. XXXX, XXX, XXX−XXX